Quantum-information processing by nuclear magnetic resonance: Experimental implementation of half-adder and subtractor operations using an oriented spin-7/2 system

K. V. R. M. Murali,[1,*] Neeraj Sinha,[1] T. S. Mahesh,[1] Malcolm H. Levitt,[3] K. V. Ramanathan,[2] and Anil Kumar[1,2,†]
[1]*Department of Physics, Indian Institute of Science, Bangalore 560012, India*
[2]*Sophisticated Instruments Facility, Indian Institute of Science, Bangalore 560012, India*
[3]*Department of Chemistry, University of Southampton, Southampton SO17 1BJ, England*
(Received 3 October 2001; published 27 August 2002)

The advantages of using quantum systems for performing many computational tasks have already been established. Several quantum algorithms have been developed which exploit the inherent property of quantum systems such as superposition of states and entanglement for efficiently performing certain tasks. The experimental implementation has been achieved on many quantum systems, of which nuclear magnetic resonance has shown the largest progress in terms of number of qubits. This paper describes the use of a spin-7/2 as a three-qubit system and experimentally implements the half-adder and subtractor operations. The required qubits are realized by partially orienting ^{133}Cs nuclei in a liquid-crystalline medium, yielding a quadrupolar split well-resolved septet. Another feature of this paper is the proposal that labeling of quantum states of system can be suitably chosen to increase the efficiency of a computational task.

DOI: 10.1103/PhysRevA.66.022313 PACS number(s): 03.67.−a

I. INTRODUCTION

Significant progress has been achieved towards the development of quantum logic [1–3] and quantum algorithms such as prime factorization [4], Deutsch-Jozsa algorithm [5,6], quantum error correction [7–10], quantum Fourier transform [11–13], and quantum database search [14–16]. The experimental implementation continues to be in early stages with nuclear magnetic resonance (NMR) demonstrating the widest applications. Several algorithms and logical operations have been implemented using both one- and two-dimensional NMR, utilizing Hamiltonian evolution [13,15–19], as well as transition selective pulses [20–28]. The operations carried out so far include single operations such as XOR, NOT, SWAP, XNOR, AND/OR, Toffoli, C^n-NOT gates [17,19,21–25,29–34], as well as multi-operation gates named ''Portmanteau Gates'' [21,24,25]. Complete set of reversible one-to-one two-qubit gates as well as many 3–5 qubit gates have been implemented [10,24,25,35,36]. Gates are the fundamental units of any arithmetic and logical operation. Combination of these gates in a given fashion gives rise to a particular arithmetic operation. Two-bit addition and subtraction are important arithmetic operations that form the basis for many computations such as multiplication and division.

Possibilities of quantum arithmetic operations such as a quantum half-adder and quantum subtractor operations have been discussed [37–39], but so far, to the best of our knowledge, not implemented experimentally. In this paper an experimental implementation of these quantum operations is carried out using a partially oriented ^{133}Cs nucleus in a liquid crystalline medium, which has a nuclear spin of 7/2, gives rise to a well-resolved quadrupolar septet and can be considered as a three-qubit system [40]. An additional feature of this paper is a demonstration that energy level labeling schemes need not follow a conventional system, but can be adopted for best efficiency for a given computation.

II. REVERSIBLE LOGIC

A. Half-adder operation

Classically a half-adder operation is defined on two bits as ''sum$=A\oplus B$'' and ''carry$=A\wedge B$,'' where $\oplus$ indicates addition modulo-2 and $\wedge$ indicates AND operation. From the truth table of this operation, given in Table I, the input to output mapping is many-to-one and is thus irreversible. Since quantum operations are carried out using unitary operations, they have to be reversible. This reversibility can be achieved by using an ancillary bit. The truth table and the circuit diagram of the half-adder using an ancillary bit are given in Table II and Fig. 1(a), respectively. In this scheme, the bit C in the input and the bit A' in the output are redundant.

B. Subtractor operation

The classical subtraction operation using two bits is also irreversible (Table I) and can be made reversible using an ancillary bit [Table II and Fig. 1(b)]. Here the bit A in the input and bit B' in the output are redundant.

It may be pointed out that Table II contains truth tables for a three-qubit system and has eight inputs and eight outputs, of which only four are needed in both half-adder and subtractor operations. The rest of the four states with $C=1$ for the half-adder operation and $A=1$ for the subtractor operation, and their outputs are not needed, but when included, give complementary carry and borrow outputs. Therefore, in effect, one obtains both the carry and borrow and their

*Present address: Media Laboratory, Massachusetts Institute of Technology, 20 Ames Street, Cambridge, MA 02139.
†Author to whom correspondence should be addressed. Email address: anilnmr@physics.iisc.ernet.in

TABLE I. Truth tables of an irreversible half-adder operation and a subtractor operation.

Input		Half-adder Output		Subtractor Output	
A	B	$A+B$	Carry	$A-B$	Borrow
0	0	0	0	0	0
0	1	1	0	1	1
1	0	1	0	1	0
1	1	0	1	0	0

complement in half-adder and subtractor operations using complete three-bit truth table of Table II. The complement may be useful for some other arithmetic operations.

III. EXPERIMENTAL IMPLEMENTATION

The implementation of quantum half-adder and subtractor operations using a spin-$\frac{7}{2}$ system by NMR is achieved using a lyotropic liquid crystal consisting of a mixture of cesium-pentadecaflouro octanoate and D_2O, which exhibits an oriented phase at 293 K.

The Zeeman Hamiltonian including the first-order quadrupolar coupling arising due to orientational order, is given by

$$\mathcal{H}=\omega_0 I_z+\frac{e^2qQ}{4I(2I-1)}(3I_z^2-I^2)S, \tag{1}$$

where $\omega_0=-\gamma B_0$ is the Larmor frequency, S the order parameter at the site of nucleus, and e^2qQ the quadrupolar coupling constant. The nuclear Zeeman energy is small compared to kT_R (where k is the Boltzmann's constant and T_R the room temperature) and the quadrupolar coupling is small compared to the Zeeman energy. Hence under high-temperature and high-field approximations, the Boltzmann distribution of populations becomes linear [41]. ^{133}Cs (spin $=7/2$) system has eight energy levels and the populations of these levels are shown on the right-hand side of Fig. 2(a), where only the differences from a uniform large background population are shown schematically. There are seven single-quantum transitions due to residual first-order quadrupole coupling [Fig. 2(a)]. The intensities of the various transitions $s_{i,i+1}$ between two successive levels i and $i+1$ are given by

$$s_{i,i+1}=(p_i-p_{i+1})|\langle i|I_x|i+1\rangle|^2, \tag{2}$$

where p_i are populations and $\langle i|I_x|i+1\rangle$ are the matrix elements of the x component of the spin-angular momentum I_x. The theoretical and experimental integrated intensity ratios are given in the caption of Fig. 2. Ratios of integrated intensities are taken since various lines have different widths (between 20 Hz and 80 Hz at half maximum) [42]. At equilibrium all p_i-p_{i+1} are equal and the theoretical intensities are proportional to $|\langle i|I_x|i+1\rangle|^2$ [Fig. 2(a)].

TABLE II. Input and output states of a reversible half-adder operation and a subtractor operation using the conventional labeling scheme.

Transition	Spin state	Input (ABC)	Output ($A'B'C'$) Half-adder	Subtractor
7	−7/2	111	100	110
6	−5/2	110	101	111
5	−3/2	101	111	001
4	−1/2	100	110	100
3	1/2	011	011	010
2	3/2	010	010	011
1	5/2	001	001	101
	7/2	000	000	000

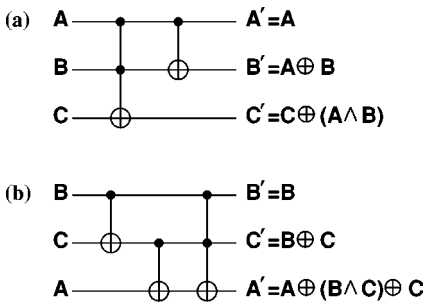

FIG. 1. Circuit diagrams of (a) reversible half-adder operation and (b) reversible subtractor operation. In the case of half-adder operation, B' is the sum and C' is the carry, and in the case of subtractor operation, C' is the subtraction and A' is the borrow.

In order to use this spin system as a three-qubit system, the various energy levels can be given different states of three qubits. One such labeling scheme is shown in the third column of Table II. Using this as input, the output of half-adder and subtractor logics are shown respectively in the fourth and fifth of Table II. To implement the half-adder operation using the labeling scheme of Table II we need to apply a cascade of population inversion (transition selective π) pulses given by the sequence

$$\text{half-adder}=\pi_7\pi_6\pi_5\pi_7\pi_6, \tag{3}$$

where the subscripts refer to the transition number given in Table II (first column) and Fig. 2(a), and the order of the pulses reads from the right to left (such that the first pulse is π_6). The half-adder operation yields the output given in the fourth column of Table II. The subtractor operator needs nine transition selective pulses in the sequence,

$$\text{subtractor}=\pi_3\pi_2\pi_3\pi_5\pi_4\pi_3\pi_2\pi_5\pi_7, \tag{4}$$

yielding the output given in the fifth column of Table II. It may be mentioned that the pulses are applied to the thermal equlibrium states and the resulting final state is read by a small-angle (10°) detection pulse to maintain linear response [25,41].

Both the sequences given above are the optimum (minimum number of pulses) with the conventional labeling scheme of Table II, in which the various energy levels are

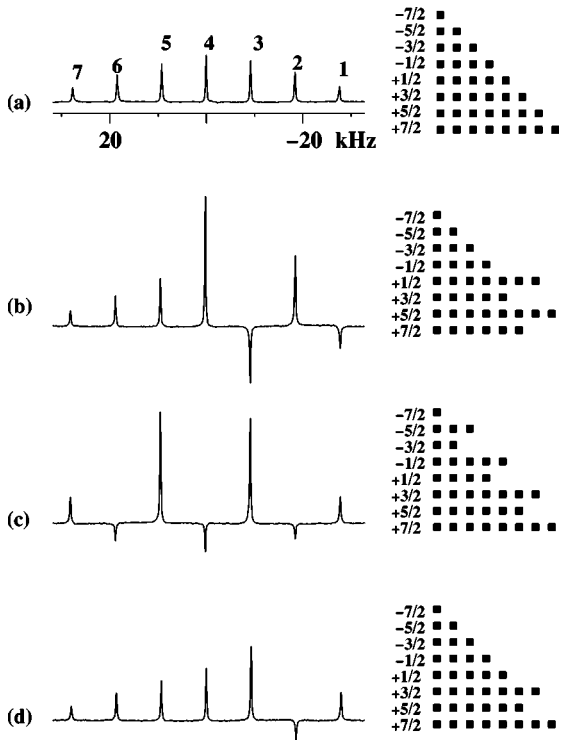

FIG. 2. (a) The equilibrium spectrum of ^{133}Cs of the lyotropic liquid crystal consisting of a mixture of cesium pentadecaflouro octanoate and D_2O at 293 K recorded at 65.59 MHz in a 11.8 T (500 MHz) NMR spectrometer. The transitions are labeled in the increasing frequency, as indicated in Table III. Also shown schematically on the right-hand side are the equilibrium populations of various energy levels. The spectra and the populations after the implementations of (b) half-adder [Eq. (5)], (c) subtractor [Eq. (6)], and (d) C^2-NOT gate (implemented by a single transition selective π pulse on transition 2). The theoretical (THEORY) and experimental (EXPT) integrated intensities of the equilibrium spectrum (a) and spectra obtained after the implementation of the logic operations (b)–(d) are (a) THEORY: (7.0):(12.0):(15.0):(16.0):(15.0):(12.0):(7.0), EXPT: [(6.9):(11.8):(15.2):(15.8):(14.8):(12.1):(7.0)]; (b) THEORY: (7.0):(12.0):(15.0):(48.0):(−30.0):(36.0):(−14.0), EXPT: [(7.3):(12.7):(18.0):(49.0):(−25.3):(34.5):(−12.5)]; (c) THEORY: (14.0):(−12.0):(45.0):(−16.0):(45.0):(−12.0):(14.0), EXPT: [(14.7):(−9.7):(50.0):(−13.5):(51.7):(−9.5):(14.3)]; (d) THEORY: (7.0):(12.0):(15.0):(16.0):(30.0):(−12.0):(14.0), EXPT: [(7.0):(12.6):(15.6):(17.8):(27.8):(−9.2):(12.7)]. Most of the errors are within 10%. The errors are mainly due to rf inhomogeneity and pulse imperfections. The transition selective π pulses were of Gaussian shape and of duration of 500 μs. The rf power was adjusted for each transition to obtain a selective π inversion. A gradient pulse of 1 ms was used after the last π pulse, to remove unwanted coherences created due to pulse imperfections. The above spectra were obtained by using a small-angle (10°) detection pulse after the implementation of the logical operations. In each spectrum, the linewidths at half maximum vary between 20 Hz and 80 Hz. All the spectra are shown after a Lorentzian line-broadening function with 200-Hz broadening.

labeled according to the increasing energy [40]. However, from a computational point of view, there is no compelling reason to follow only the above labeling scheme. Any scheme should be equally valid provided only one label is attached to each energy level, and once a labeling scheme has been chosen, it is consistently maintained throughout a set of computations. It is therefore permitted to choose a labeling scheme that is most efficient for the desired set of computations. It is obvious that different labeling schemes are efficient for different sets of computations. An alternate labeling scheme is suggested in Table III. The spin states and transition numbers, like in Table II, are in increasing energy levels from the bottom to top, but the labeling of the levels in the third column, is different from that of Table II. With this modified labeling scheme (Table III), the half-adder operation is achieved by the sequence,

$$\text{half-adder} = \pi_1 \pi_3 \pi_2 , \tag{5}$$

and the subtractor by

$$\text{subtractor} = \pi_2 \pi_4 \pi_6 . \tag{6}$$

This leads to the optimum labeling for implementation of half-adder and subtractor operations for the present system. The experimental implementation of the operations are given in Figs. 2(b) and 2(c), respectively. The final populations are shown schematically on the right-hand sides (rhs), and the corresponding spectra, shown on the left-hand sides (lhs) of Fig. 2. The modified populations are the result of the three unitary transforms corresponding to the implemented circuit in each case. For example, for the half-adder [Fig. 2(b)], the first π pulse on transition 2 exchanges the populations of levels +3/2 and +5/2, the second π pulse on transition 3 exchanges the populations of levels +3/2 and +1/2 and finally the last π pulse on transition 1 exchanges the populations of levels +7/2 and +5/2. Thus the cascade of the above three selective π pulses results in the population redistribution as shown on the rhs in the Fig. 2(b). Such a population distribution results in a spectrum obtained by using a small-angle (10°) pulse, as shown on the lhs of Fig. 2(b). The theoretically expected intensity ratios after the half-adder operation are (7.0):(12.0):(15.0):(48.0):(−30.0):(36.0):(−14.0), while the observed intensity ratios are (7.3):(12.7):(18.0):(49.0):(−25.3):(34.5):(−12.5). This

TABLE III. Input and output states of a half-adder and subtractor using an optimized labeling scheme The circuit diagrams of half-adder and subtractor operations are shown in Fig. 1. The output of the Toffoli (C^2-NOT) gate is $A'=A, B'=B, C'=C\oplus(A\wedge B)$.

Transition	Spin state	Input (ABC)	Output ($A'B'C'$) Half-adder	Subtractor	C^2-NOT
7	−7/2	000	000	000	000
6	−5/2	010	010	011	010
5	−3/2	011	011	010	011
4	−1/2	001	001	101	001
3	1/2	101	111	001	101
2	3/2	110	101	111	111
1	5/2	111	100	110	110
	7/2	100	110	100	100

confirms the half-adder operation. For the subtractor operation the three transition selective pulses commute and can be applied in any order. Starting from the equilibrium population shown in Fig. 2(a), the π_6 exchanges the population of $-5/2$ and $-3/2$ levels, the π_4 those of $-1/2$ and $1/2$ levels and the π_2 those of levels $+3/2$ and $+5/2$, respectively, resulting in the populations shown on the right-hand side of Fig. 2(c). These, measured by a small-angle (10°) pulse, yield the spectrum shown on the lhs of Fig. 2(c). The theoretically expected intensity ratios are (14.0):(−12.0):(45.0):(−16.0):(45.0):(−12.0):(14.0), and the observed ratios are, (14.7):(−9.7):(50.0):(−13.5):(51.7):(−9.5):(14.3), confirming the subtractor operation. It may be mentioned that π_3 and π_1 in half-adder operation, and all the pulses of the subtractor operation, commute and can be applied simultaneously, using a modulator. Thus the half-adder operation reduces to two noncommuting operations and the subtractor to a single operation.

The result of a Toffoli gate can also be easily implemented with the new labeling scheme. Table III contains the result of a C^2-NOT operation on the third qubit. This is achieved experimentally by a single-transition selective π_2 pulse and the result is shown in Fig. 2(d). It may be mentioned that the C^2-NOT on the third qubit can also be easily achieved with the conventional labeling of Table II by using a π_7 pulse.

IV. CONCLUSIONS

This paper describes the use of an oriented spin-7/2 as a three-qubit system. Using such a system, the quantum half-adder, subtractor, and C^2-NOT operations have been experimentally implemented by utilizing transition selective inversion pulses. The number of pulses needed for these operations have been minimized by an optimized labeling of the eigenstates of the spin system. In strongly coupled spins, the identification of a spin as a qubit no longer holds. In such cases one can still carry out various logical operations with arbitrary labeling schemes, as will be shown elsewhere [43].

ACKNOWLEDGMENTS

We thank Dr. J.P. Bayle, Université de Paris-Sud, Orsay, France for providing the liquid crystal sample. K.V.R.M.M. would like to thank the Department of Science and Technology, New Delhi, for financial support. The authors also acknowledge the use of a 500-MHz FT-NMR spectrometer of the Sophisticated Instruments Facility, Indian Institute of Science, funded by the Department of Science and Technology, New Delhi.

[1] R.P. Feynmann, Int. J. Theor. Phys. **21**, 467 (1982).
[2] C.H. Bennett, Int. J. Theor. Phys. **21**, 905 (1982).
[3] D. Deutsch, Proc. R. Soc. London, Ser. A **400**, 97 (1985).
[4] P.W. Shor, SIAM J. Comput. **26**, 1484 (1997).
[5] D. Deutsch and R. Jozsa, Proc. R. Soc. London, Ser. A **439**, 553 (1992).
[6] R. Cleve, A. Ekert, C. Macchiavello, and M. Mosca, Proc. R. Soc. London, Ser. A **454**, 339 (1998).
[7] P. Shor, Phys. Rev. A **51**, 992 (1995).
[8] A. Steane, Phys. Rev. Lett. **77**, 793 (1996).
[9] E. Knill and R. Laflamme, Phys. Rev. A **55**, 900 (1997).
[10] E. Knill, R. Laflamme, R. Martinez, and C. Negrevergne, Phys. Rev. Lett. **86**, 5811 (2001).
[11] D. Coppersmith, IBM Research Report No. RC19642, 1994.
[12] A. Ekert and R. Jozsa, Rev. Mod. Phys. **68**, 733 (1996).
[13] Y.S. Weinstein, M.A. Pravia, E.M. Fortunato, S. Lloyd, and D.G. Cory, Phys. Rev. Lett. **86**, 1889 (2001).
[14] L.K. Grover, Phys. Rev. Lett. **79**, 325 (1997).
[15] I.L. Chuang, N. Gershenfeld, and M. Kubinec, Phys. Rev. Lett. **80**, 3408 (1998).
[16] J.A. Jones, M. Mosca, and R.H. Hansen, Nature (London) **393**, 344 (1998).
[17] D.G. Cory, M.D. Price, and T.F. Havel, Physica D **120**, 82 (1998).
[18] J.A. Jones and M. Mosca, J. Chem. Phys. **109**, 1648 (1998).
[19] Z.L. Madi, R. Bruschweiler, and R.R. Ernst, J. Chem. Phys. **109**, 10 603 (1998).
[20] N. Linden, H. Barjat, and R. Freeman, Chem. Phys. Lett. **296**, 61 (1998).
[21] Kavita Dorai, Arvind, and Anil Kumar, Phys. Rev. A **61**, 042306 (2000).
[22] Kavita Dorai, T.S. Mahesh, Arvind, and Anil Kumar, Curr. Sci. **79**, 1447 (2000).
[23] A.K. Khitrin and B.M. Fung, J. Chem. Phys. **112**, 6963 (2000).
[24] T.S. Mahesh, Kavita Dorai, Arvind, and Anil Kumar, J. Magn. Reson. **148**, 95 (2001).
[25] Neeraj Sinha, T.S. Mahesh, K.V. Ramanathan, and Anil Kumar, J. Chem. Phys. **114**, 4415 (2001).
[26] Arvind, Kavita Dorai, and Anil Kumar, Pramana, J. Phys. **56**, L705 (2001).
[27] Kavita Dorai, Arvind, and Anil Kumar, Phys. Rev. A **63**, 034101 (2001).
[28] T.S. Mahesh and Anil Kumar, Phys. Rev. A **64**, 012307 (2001).
[29] J.A. Jones, R.H. Hansen, and M. Mosca, e-print quant-ph/9805070.
[30] J. Du, M. Shi, J. Wu, X. Zhou, and R. Han, Phys. Rev. A **63**, 042302 (2001).
[31] M.D. Price, T.F. Havel, and D.G. Cory, Phys. Rev. A **60**, 2777 (1999).
[32] X. Zhou, D.W. Leung, and I.L. Chuang, Phys. Rev. A **62**, 052316 (2000).
[33] E. Dennis, Phys. Rev. A **63**, 052314 (2001).
[34] X. Wang, A. Sorensen, and K. Molmer, Phys. Rev. Lett. **86**, 3907 (2001).
[35] R. Marx, A.F. Fahmy, J.M. Myers, W. Bermel, and S.J. Glaser, Phys. Rev. A **62**, 012310 (2000).
[36] L.M.K. Vandersypen, M. Steffen, G. Breyta, C.S. Yannoni, R.

Cleve, and I.L. Chuang, Phys. Rev. Lett. **85**, 5452 (2000).
[37] V. Vedral, A. Barenco, and A. Ekert, Phys. Rev. A **54**, 147 (1996).
[38] P. Gossett, e-print quant-ph/9808061.
[39] T.G. Draper, e-print quant-ph/0008033.
[40] A. Khitrin, H. Sun, and B.M. Fung, Phys. Rev. A **63**, 020301(R) (2001).
[41] R.R. Ernst, G. Bodenhausen, and A. Wokaun, *Principles of Nuclear Magnetic Resonance in One and Two Dimensions* (Oxford University Press, Oxford, 1987).
[42] A. Abragam, *The Principles of Nuclear Magnetism* (Oxford University Press, Oxford, 1961).
[43] T.S. Mahesh, Neeraj Sinha, Malcolm H. Levitt, K.V. Ramanathan, and Anil Kumar (unpublished).